



**Eva Rajo-Iglesias**

Departamento de Teoría de la Señal y Comunicaciones  
University Carlos III of Madrid  
Despacho 4.3B10  
Avenida de la Universidad,  
30, 28911 Leganés, Madrid, Spain  
Tel: +34 91 624 8774;  
Fax: +34 91 624 8749  
E-mail: eva@tsc.uc3m.es

# Evaluation of the Quality Factor, $Q$ , of Electrically Small Microstrip-Patch Antennas

*Georgios A. Mavridis<sup>1</sup>, Dimitris E. Anagnostou<sup>2</sup>, and Michael T. Chryssomallis<sup>1</sup>*

<sup>1</sup>Department of Electrical and Computer Engineering, Microwaves Laboratory  
Democritus University of Thrace  
Gr-67100 Xanthi, Greece  
E-mail: mchryss@ee.duth.gr

<sup>2</sup>Department of Electrical & Computer Engineering  
South Dakota School of Mines and Technology  
Rapid City, SD 57701-3995, USA

---

## Abstract

The quality factor,  $Q$ , for a number of configurations of a microstrip antenna is evaluated using exact and approximate quality-factor formulas found in the literature. A number of slits parallel to the radiating edges are used to miniaturize the microstrip antenna's size. The microstrip antenna in use is considered to be electrically small according to Wheeler's electrically small antenna definition. The  $Q$  for each configuration is numerically evaluated using the given expressions, for simulated and measured data, and is compared to the Chu lower bound. There is good agreement between the results, while the  $Q$  lower fundamental limitation is not violated. Despite the size reduction, satisfying radiation efficiency is achieved, and the radiation pattern remains unchanged.

Keywords: Chu limit; electrically small antennas; microstrip antennas; quality factor  $Q$

## 1. Introduction

Today, there is a demand in modern communication systems for smaller antennas, with sizes significantly less than the usual half-wavelength. However, the antenna's size with respect to the wavelength is the parameter that will have the main influence on the radiation characteristics, thus making the miniaturization process a challenging task. Antennas can be made smaller by increasing their electrical length, without affecting their physical length.

The purpose of this work is twofold. The first purpose is to investigate the miniaturization of a rectangular microstrip-patch antenna by inserting a number of slits parallel to the radiating edges (as these are defined for a rectangular microstrip). The slits force the surface currents to meander, thus artificially increasing the antenna's electrical length, without modifying the patch's global dimensions. A significant decrease in the resonant frequency is observed, depending on the slit's length and width. The resultant antenna can be characterized as a small antenna in accordance with the relevant

fundamental limitations. Second, there are a number of exact and approximate expressions found in the literature [1-4] used to calculate the quality factor,  $Q$ , primarily for but not limited to wire antennas. In this work, these formulas are applied to the proposed miniaturized microstrip antennas to check the antennas' behavior and the validity under these formulas. The presented numerical results are compared to the Chu limit concerning the lowest achievable quality factor,  $Q$ , as a function of the antenna's occupied physical volume.

## 2. $Q$ Definitions and Fundamental Limits

As a measure of antenna performance, the quality factor can generally be defined in three ways: (i) as a relation between the stored reactive energy and the radiated power of the antenna, (ii) as a function of its impedance or admittance, and (iii) as a function of its bandwidth. Every approach has its own physical meaning and yields different operational limits.

Using the first approach, for a nonresonant antenna that is tuned by a lossless reactive element so that its input impedance becomes purely real, an exact quality factor of the system consisting of the antenna and the ideal reactive element can be defined as [5, 6]

$$Q = \frac{2\omega_0 W}{P}, \quad (1)$$

where  $\omega_0$  is the angular resonant frequency,  $W$  is the larger of the time-averaged stored magnetic and electric energies in the antenna, and  $P$  is the total power dissipated in radiation and losses. Consequently, Equation (1) can be considered to be the upper bound on the  $Q$  of an antenna system that is tuned to resonance by the addition of a single reactive element. Any loss in the tuning element would reduce the  $Q$  below that given by Equation (1).

Equation (1) calculates the exact value of  $Q$  of an antenna, and requires that internal energy and dissipated power be expressed in terms of the antenna's field properties and impedance. According to [1], the definition in Equation (1) for the quality factor,  $Q$ , of an electrically small antenna can be expressed as

$$Q(\omega_0) = \left| \frac{\omega_0}{2R_0(\omega_0)} X'_0(\omega_0) - \frac{2\omega_0}{|I_0|^2 R_0(\omega_0)} [W_L(\omega_0) + W_R(\omega_0)] \right| \quad (2)$$

where  $R_0(\omega_0) = R(\omega_0)$  is the input resistance of the antenna,  $X_0(\omega_0) = X(\omega_0) + X_s(\omega_0)$  is the total input reactance ( $X_s(\omega_0)$  is the reactance of the ideal tuning element at the resonant frequency),  $I_0$  is the total current amplitude,  $W_L(\omega_0)$  is the material-loss dispersion energy, and  $W_R(\omega_0)$  is the far-field dispersion energy, where dispersion means that these

energies depend on the frequency derivative of the fields. All the necessary relations for the evaluation of the above quantities can be found in [1]. The expressions on the right-hand sides of Equations (1) and (2) are very different in form, yet they are exact, and thus produce the same value of  $Q(\omega_0)$ .

Following the second approach, the quality factor of an electrically small antenna – which is characterized by a single impedance resonance within a defined bandwidth of interest – can be approximated at any angular frequency  $\omega$  by [1]

$$Q_z(\omega) \approx \frac{\omega}{2R(\omega)} \sqrt{R'(\omega)^2 + \left[ X'(\omega) + \frac{|X(\omega)|}{\omega} \right]^2}, \quad (3)$$

where  $R(\omega)$  and  $X(\omega)$  are the input resistance and reactance of the antenna, respectively, and the prime denotes a frequency derivative.

Beyond these exact and approximate expressions of the antenna's  $Q$ , which take into account the antenna's field properties and impedance, from the third approach follows an expression that relates  $Q$  to the matched voltage-standing-wave-ratio (VSWR) bandwidth. For an antenna tuned at a frequency  $\omega_0$ , this bandwidth is defined as the difference between the two frequencies on either side of  $\omega_0$  at which the VSWR equals a constant value,  $s$ , provided the characteristic impedance,  $Z_0$ , of the feed line is equal to  $Z_0(\omega_0) = R_0(\omega_0) = R(\omega_0)$ . The relationship between the two quantities is finally given by [1]

$$FBW_V(\omega_0) = \frac{\omega_+ - \omega_-}{\omega_0},$$

$$Q_{FBW_V}(\omega_0) \approx \frac{2\sqrt{\beta}}{FBW_V(\omega_0)}, \quad (4)$$

$$\sqrt{\beta} = \frac{s-1}{2\sqrt{s}} \leq 1.$$

The expression in Equation (4), as well as the aforementioned exact Equation (2) and the approximate Equation (3) expressions, are used here to calculate the quality factor,  $Q$ , of the miniaturized microstrip-antenna configurations. The results are compared with the Chu limitation and the miniature antenna limit in Section 3. For a stricter bound, especially for well-defined (Euclidean) antenna shapes, one can also use the expression given in [7]. In addition, this work extends and validates previous results [8, 9] with measurements for traditional and meander microstrip antennas.

While the exact expression of Equation (1) for the antenna's  $Q$  defines an upper bound for its value [6], a restriction is also imposed concerning its lower value for a given antenna. The fundamental  $Q$  limitations of small antennas

were first addressed by Wheeler [10-12] and Chu [5]. It has been shown that when an antenna becomes electrically small, its bandwidth decreases. Chu related the antenna's radiation quality factor,  $Q$ , to the "radiansphere," the smallest sphere that encloses the antenna [10-12]. Chu established a fundamental  $Q$  limitation, which was later reexamined by McLean [13], and is given by

$$Q = \frac{1}{k^3 a^3} + \frac{1}{ka}, \quad (5)$$

where  $\lambda$  is the operating wavelength,  $a$  is the radius of the radiansphere, and  $k = 2\pi/\lambda$ .

For a rectangular microstrip antenna with (finite) dielectric only underneath the patch and (ideally) infinite ground plane, the radiansphere has a radius slightly larger than half of the diagonal dimension of the patch, due to the thickness of the substrate. The expression in Equation (5) holds for linearly polarized antennas, and establishes a fundamental limit that no antenna can ever exceed, independently of the art that is used to construct it. If the antenna has losses, meaning the efficiency is lower than unity, then  $Q_{lb} = \eta Q$ . Thus, the more efficiently an antenna occupies its radiansphere, the closer its  $Q$  would be to the lower Chu bound, while an improved bandwidth can be achieved [14, 15].

Wheeler and Chu also introduced the definition of the *electrically small antenna* (ESA). An antenna is considered to be electrically small if the radius of its radiansphere is  $a < \lambda/2\pi$ , or, alternatively, if  $ka < 1$ . However, small antennas are subject to a number of limitations and restrictions that cause their performance to deteriorate. While the radiation pattern of a small antenna remains practically the same for a smaller size, the radiation resistance decreases relative to other resistances (ohmic losses, dielectric losses). This results in reduced efficiency, and is one of the principal limitations of electrically smaller antennas.

### 3. Numerical Results

A rectangular microstrip-patch antenna of resonant length  $L = 36$  mm and width  $W = 44$  mm was initially designed on Rogers™ RO3003 substrate, with  $\epsilon_r = 3.00$  and  $\tan \delta = 0.0013$ . With this patch as a basis, meander microstrip antennas that had the same overall patch dimensions were also designed and fabricated on three substrates of different thickness:  $h = 0.75$  mm,  $h = 1.5$  mm, and  $h = 3$  mm. The schematics of these patches are shown in Figure 1. The slits for the meander patches were placed parallel to the radiating edges of the rectangular patch ( $W$ ); when this resonates at the fundamental mode, they achieve an area miniaturization as they force the current on the surface of the patch to follow a meander route. This increases the electrical length and decreases the antenna's resonant frequency,  $f_r$ , while its overall dimensions remain unchanged. The above statement is expressed using the quantity

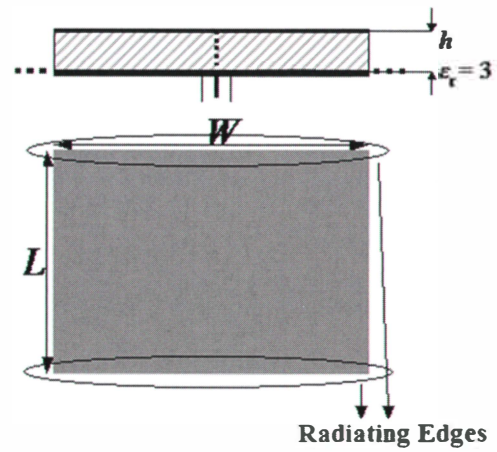


Figure 1a. The original patch antenna utilized.

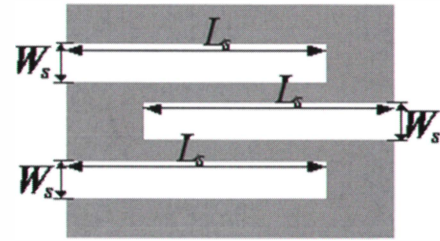


Figure 1b. The layout of the resultant small antenna.

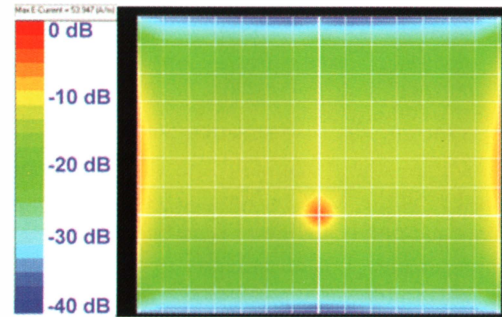


Figure 2a. The current distribution for the basic rectangular patch.

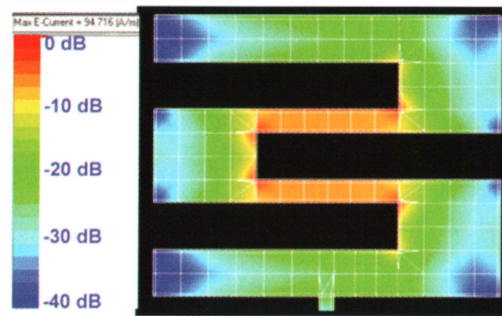


Figure 2b. The current distribution for the patch design with a slit length of  $L_s = 31$ .

known as electrical size,  $E_s = L/\lambda$ , and so as  $L_s$  (the slit length) increases, the electrical size diminishes. This miniaturization procedure becomes apparent in Figure 2, which shows the average current density distribution for both configurations. In Figure 2b, a maximum current density is shown, located at the center of the patch, because the whole current is forced to flow from one edge to the other, passing

**Table 1. 3 mm coaxially fed meander microstrip antennas: slit length, resonant frequency, measured and simulated approximate  $Q_z$  from Equation (3), measured matched VSWR bandwidth  $Q_{FBW}$  from Equation (4) for  $SWR = 2$ , simulated exact  $Q_0$  from Equation (2), electrical size, radiansphere radius and product  $ka = 2\pi a/\lambda_0$ , and simulated radiation efficiency.**

$L_s$ (mm)	$f_0$ (GHz)	$Q_z$ (Meas.)	$Q_z$ (Simul.)	$Q_{FBW}$ ( $SWR = 2$ )	$Q_{exact}$ (Simul.)	$E_s$ ( $L/\lambda_g$ )	$a/\lambda_0$	$ka$	Radiation Efficiency (%)
0	2.236	29.5	26.4	28.6	25.8	0.444	0.212	1.331	83.1
13	1.665	–	92.0	–	–	0.331	0.158	0.991	71.8
15	1.535	–	112.6	–	–	0.305	0.145	0.914	63.8
17	1.400	158.3	132.6	155.4	132	0.278	0.133	0.834	53.3
19	1.263	194.6	173.6	188.8	167	0.251	0.120	0.752	40.2
21	1.115	–	150.0	–	–	0.222	0.106	0.664	24.6
23	0.953	–	200.7	–	–	0.190	0.090	0.567	21.5
25	0.838	–	223.6	–	–	0.167	0.080	0.499	11.1
27	0.755	–	248.4	–	–	0.150	0.072	0.449	5.7
29	0.689	–	286.3	–	–	0.137	0.065	0.410	3.7
31	0.64	–	361.6	–	–	0.123	0.061	0.381	2.4

**Table 2. A comparison among coaxially fed meander antennas: slit length, resonant frequency, and simulated radiation efficiency.**

$L_s$ (mm)	$f_0$ (GHz)	Radiation Efficiency (%)	$f_0$ (GHz)	Radiation Efficiency (%)	$f_0$ (GHz)	Radiation Efficiency (%)
0	2.36	71.0	2.32	82.7	2.24	83.1
17	1.33	9.2	1.36	25.7	1.40	53.3
19	1.17	4.6	1.21	15.6	1.26	40.2
31	0.54	0.1	0.58	0.3	0.64	2.4

only through this narrow path. After a number of simulations, the slit width,  $W_s$ , was set equal to 6 mm, while the increase of the slit length,  $L_s$ , can significantly shift the resonant frequency downwards. Simulations were carried out using *IE3D*<sup>TM</sup>, a commercial Method of Moments (MoM) code well suited for planar structures.

The responses of antennas designed with  $h = 0.75$  mm, with slit lengths equal to  $L_s = 21, 23, 25, 27, 29$ , and 31 mm, are shown in Figure 3. In this case, the resonant frequency shifted from 2.36 GHz for the rectangular patch or patch with  $L_s = 0$  mm, down to 0.54 GHz for the  $L_s = 31$  mm case. Similar results were also obtained for the other substrate thicknesses, as the first two columns of Table 1 show for the case of the 3 mm substrate. Such a procedure corresponds to a frequency reduction and thus a size reduction, which is important in situations where space is a significant design constraint [16, 17]. In addition, it can lead to a metallization-area reduction,

which facilitates the printing of these antennas using low-cost direct-write-deposition methods [18]. Nevertheless, the achieved frequency reduction is related to an extreme radiation-efficiency reduction, which makes most of the proposed meander antennas useless, especially those designed on the thin substrates of 0.75 and 1.5 mm. As can be seen in Table 2 – where three characteristic slit lengths were chosen to be shown, i.e., 17, 19, and 31 mm – for the three substrate thicknesses used, the achieved radiation efficiency had good values only for the case of the 3 mm substrate. The extremely low values of radiation efficiency for the substrates with 0.75 and 1.5 mm thicknesses were confirmed with measurements of fabricated prototypes. For this reason, we chose to show results only for the case of the 3 mm-thick substrate.

The quality factor,  $Q$ , from Equations (2) to (4) was calculated from simulations for all the antenna configurations. The real and imaginary parts of the simulated input impedances,



$\text{Re}(Z_{in})$  and  $\text{Im}(Z_{in})$ , were extracted from the simulation results for a frequency range from 0.5 to 2.5 GHz, and used in Equations (2) and (3). The VSWR simulation results were used in Equation (4), which relates the  $Q$  to the matched bandwidth.

A number of antenna prototypes, both edge-fed and coaxially fed, were chosen to be fabricated and measured in order to validate the results of the simulations. Photos of some of the fabricated prototypes are shown in Figure 4. From the results obtained, the measured  $Q_z$  of the coaxially fed antennas showed slightly better agreement with the simulated values, although the difference from the edge-fed antennas was rather small. For this reason, the presented measurement results are from the fabricated coaxially fed prototypes. The antenna's input impedance was also measured in the range from 0.5 to 2.5 GHz with a 1.25 MHz step size, and the data were used in Equations (2) and (3). Thus,  $Q_z$  for the fabricated antennas was calculated for all the frequencies in this range, not only for the resonant frequencies, and these values are shown as  $Q_z$  (Meas.) in Table 1 and Figures 5, 6, and 7. The results were compared with exact expression for  $Q$  as defined in Equation (2). The necessary integrals for the evaluation of  $W_L$  and  $W_R$  in (2) were numerically evaluated for each observation angle and frequency as necessary to accurately compute the frequency derivative with a finite difference, using the radiation-pattern data available from the simulation results. It was noteworthy that the accuracy of the simulations to obtain smooth curves was set to the 16th decimal point. Such accuracy in the measurements was not possible, since the vector network analyzer (VNA) utilized to measure the input impedance of the fabricated antennas had an accuracy of six decimal points. This is a general issue in measurement procedures, since there is no vector network analyzer that can give such high decimal-point accuracy as in the simulations.

In contrast to wire antennas, which are placed in free space and are characterized with the help of the free-space wavelength,  $\lambda_0$ , microstrip-antenna dimensions are typically related to the guide wavelength,  $\lambda_g$ . The length of the resonance path in terms of this  $\lambda_g$  determines the resonant frequency. On the other hand, the fields of the microstrip antennas are created from within a dielectric volume and are radiated into free space. The volume where the fields are radiated is thus related to  $\lambda_0$ . This is because in radiation problems, the radiation ability of an antenna – electrically small antennas included – is evaluated by how much energy can be transmitted to free space, which is associated with  $\lambda_0$ . The antenna is rather small, and the volume it takes can almost be omitted at the observing point in the far-field area, no matter what material is used to design the antenna. The seventh column of Table 1 summarizes (for  $h = 3$  mm) the electrical size,  $E_s$ , for each slit case in terms of the guide wavelength,  $\lambda_g$ . The radiansphere radius,  $a$ , and the product  $ka$ , which are used in order to define an antenna as electrically small, are expressed in terms of  $\lambda_0$  (in the eighth and ninth columns). All cases presented adhered to the fact that the ratio of the antenna's largest dimension to the resonant wavelength

was such that the product  $ka$  was below the Chu limit concerning the small-antenna definition ( $ka < 1$ ). All designed meander antennas could thus be characterized as “small antennas.”

The results showed that the simulations were close to the measurements, which validated that the equations can be successfully used with meander-shaped microstrip antennas. In general, there was very good agreement between the results using the approximate Equations (3) and (4), and the exact Equation (2), definitions of  $Q$ . For all the presented cases, the exact  $Q$  and the approximate  $Q$  results were well above the established lower limit for  $Q$ . From the simulated  $Q_z$  results, it was apparent that there was a steady increase in  $Q$  as the slit length increased and the antenna became electrically smaller. This was expected, since as the antenna diminished electrically, its fractional bandwidth became narrower, which led to high  $Q$  values according to Equation (4). For the selected meander cases of  $L_s = 17$  mm and  $L_s = 19$  mm on a substrate thickness of 3 mm – which were electrically small antennas and presented radiation efficiencies equal to 53.3% and 40%, respectively – the measured  $Q_z$ , calculated using Equation (3), and the values of the measured antenna input impedance,  $\text{Re}(Z_{in})$  and  $\text{Im}(Z_{in})$ , are shown in Table 1. As could be seen, there was good agreement between the simulated and measured  $Q_z$ . This agreement was better for the rectangular case, where the deviation was only 10%, and it deteriorated for the  $L_s = 19$  mm meander case, where it became 22%. This fact may be attributed to the ripple of the measured  $Q_z$  due to the limited accuracy of the vector network analyzer, which became more pronounced as the frequency decreased.

In Figures 5, 6, and 7, the superimposed simulated and measured  $Q_z$  curves obtained using the approximate expression of Equation (3) for the 3 mm coaxially fed rectangular ( $L_s = 0$  mm) microstrip antenna, and for the meandered microstrip antennas with  $L_s = 17$  mm and  $L_s = 19$  mm, are depicted. They are also compared to the Chu  $Q$  limit for the lossless case

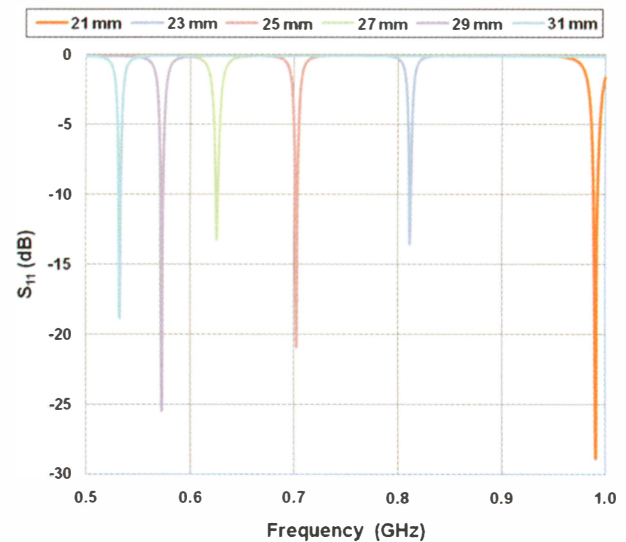


**Figure 3. The simulated return loss (in dB) for the antenna with slits as a function of the slit length,  $L_s$ .**

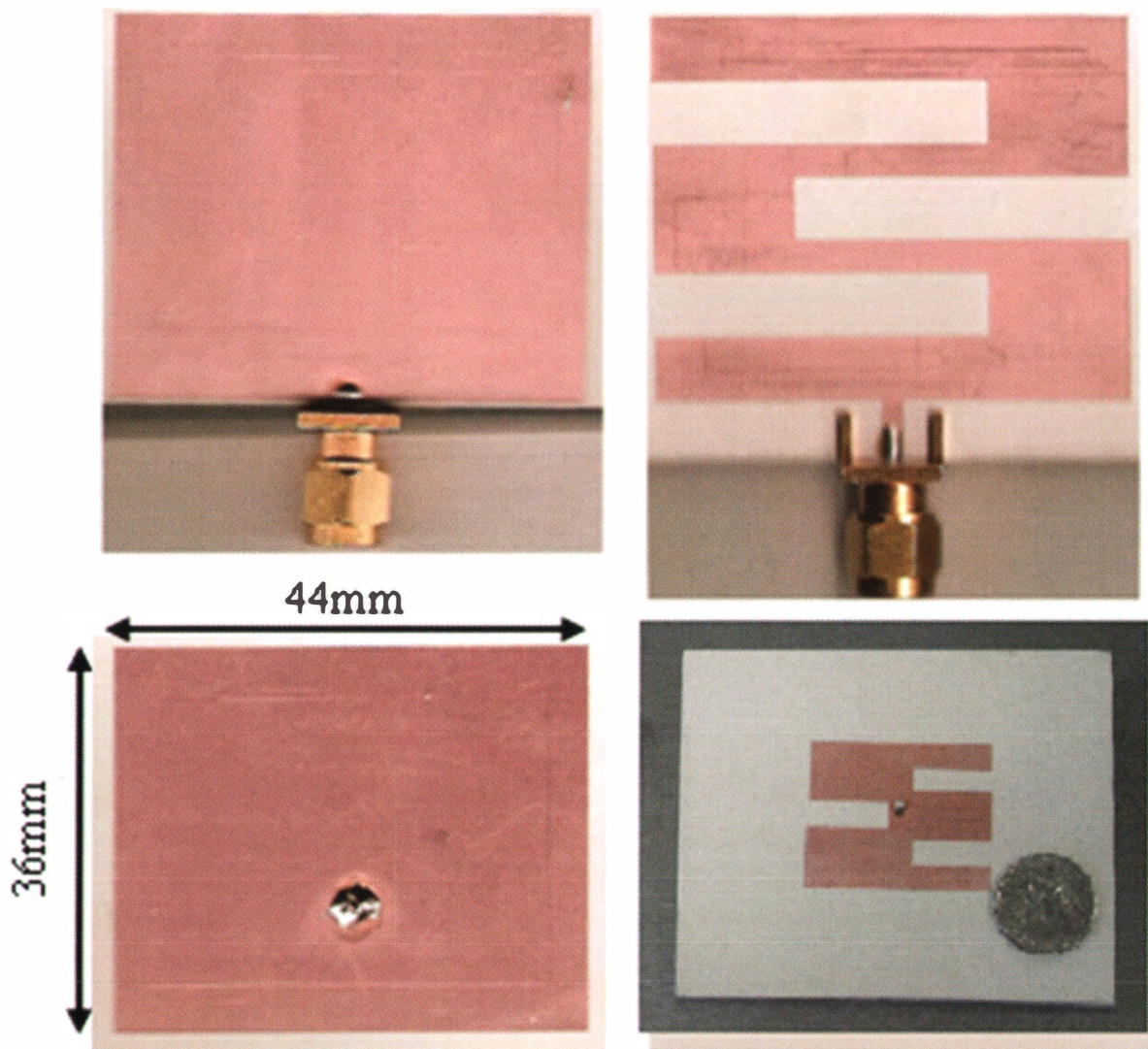


Figure 4. Photos of some fabricated prototypes of rectangular (edge-fed and coaxially fed, and slotted (edge-fed and coaxially fed) microstrip antennas on RO3003 substrate. Note that the patch area was always the same: 44 mm × 36 mm.

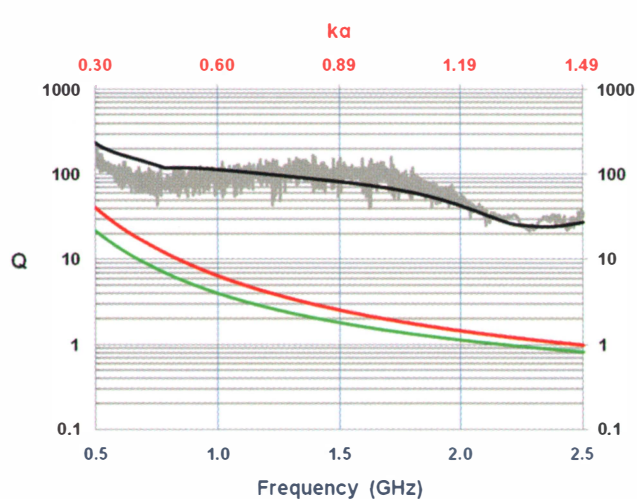


Figure 5. The measured (gray) and simulated (black) values of  $Q_z$  for the 3 mm-thick coaxially fed rectangular microstrip antenna, along with the curves for the lower bound,  $Q_{lb}$ , for linear polarization (red), and the  $Q_{lb}$  for circular polarization (green). The antenna resonated at 2.24 GHz.

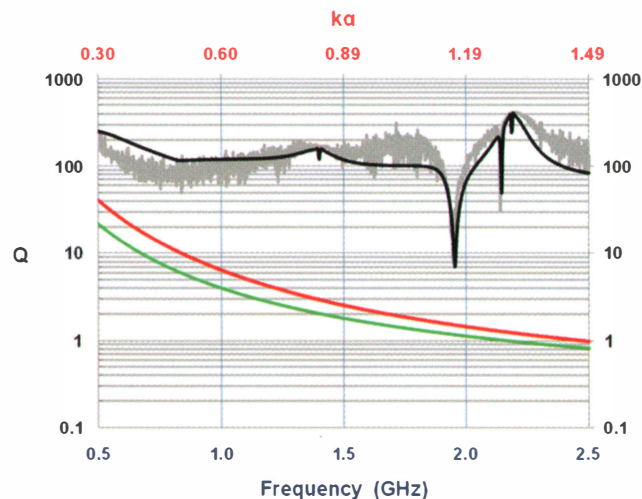
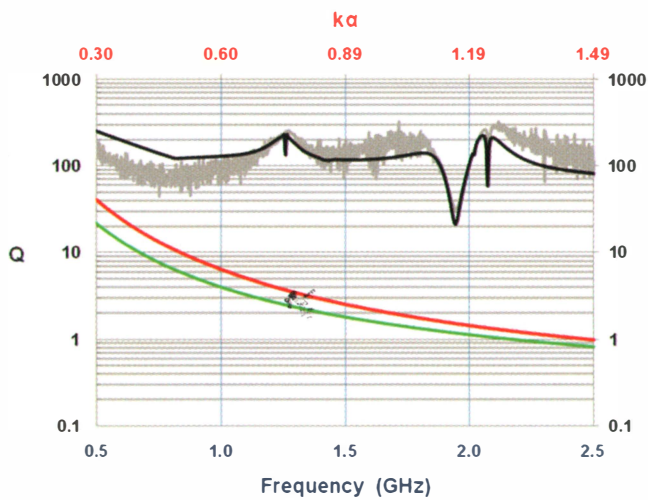
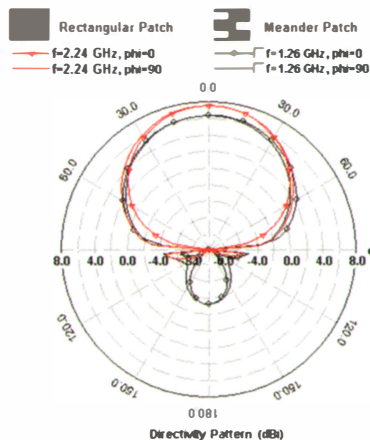


Figure 6. The measured (gray) and simulated (black) values of  $Q_z$  for the 3 mm-thick coaxially fed meander microstrip antenna with  $L_s = 17$  mm, along with the curves for the lower bound,  $Q_{lb}$ , for linear polarization (red) and the  $Q_{lb}$  for circular polarization (green). The resonance occurred at 1.4 GHz.





**Figure 7.** The measured (gray) and simulated (black) values of  $Q_z$  for the 3 mm-thick coaxially fed meander microstrip antenna with  $L_s = 19$  mm, along with the curves for the lower-bound,  $Q_{lb}$ , for linear polarization (red) and the  $Q_{ib}$  for circular polarization (green). The resonance occurred at 1.26 GHz.



**Figure 8.** The simulated antenna directivity radiation patterns (dBi) in the elevation plane ( $\varphi = 0^\circ$ ,  $\varphi = 90^\circ$ ) for the rectangular patch and the meander patch with slit lengths  $L_s = 19$  mm.

for linear and circular polarization. The circular-polarization curve is shown only for completeness purposes. The radiated fields of the rectangular and meander patch antennas were simulated for all the aforementioned configurations. As was expected, no distortion was observed in the shape of the radiation patterns between the rectangular and the resultant small meander antennas. In Figure 8, the directivity pattern of the case with a slit length of 19 mm on the 3 mm-thick substrate was chosen to be shown, in comparison with that of the rectangular patch, to show that the radiation pattern remained practically unchanged.

#### 4. Conclusion

A basic rectangular microstrip-patch antenna can be miniaturized by inserting a number of slits parallel to the radi-

ating edges (of a rectangular microstrip). The resultant antennas with slits can be characterized as “small antennas,” since the Chu and Wheeler limits are satisfied. The quality factor,  $Q$ , for all configurations was numerically calculated using exact and approximate  $Q$  expressions, along with the inverse bandwidth and  $Q$  relations. Good agreement among the results was observed, indicating a successful application of these quality-factor formulas on electrically small microstrip antennas. A frequency reduction of up to 80% and an area reduction up to 44% were observed, depending on the length of the slit. Miniaturized antennas with dimensions comparable to  $\lambda_0/10$  or smaller were fabricated and measured. It was noticed that as the slit length was increased for a given substrate thickness, there was deterioration in the antenna’s radiation efficiency. However, by increasing the thickness of the substrate while the overall antenna dimensions remained unchanged, a radiation efficiency close to 50% could be achieved, in combination with a 50% reduction in the resonant frequency. The resultant antennas could still be characterized as electrically small, since the product  $ka < 1$ , according to the Chu and Wheeler limits. Further work is currently being carried out to increase the efficiency of such antennas, using structural modifications or dielectric superstrates.

#### 5. Acknowledgement

This material was based in part upon work supported by the DARPA/MTO Young Faculty Award N66001-11-1-4145, the Army Research Office Grant W911NF-09-1-0277, NASA SD EPSCoR under Cooperative Agreement NNX07AL04A, and NSF Grant Proposals ECS-0824034 and EPS-0903804.

#### 6. References

1. A. D. Yaghjian and S. R. Best, “Impedance, Bandwidth, and  $Q$  of Antennas,” *IEEE Transactions on Antennas and Propagation*, **AP-53**, 4, April 2005, pp. 1298-1324.
2. S. R. Best, “Low  $Q$  Electrically Small Linear and Elliptical Polarized Spherical Dipole Antennas,” *IEEE Transactions on Antennas and Propagation*, **AP-53**, 3, March 2005, pp. 1047-1053.
3. S. R. Best, “A Discussion on Quality Factor of Impedance Matched Electrically Small Wire Antennas,” *IEEE Transactions on Antennas and Propagation*, **AP-53**, 1, January 2005, pp. 502-508.
4. S. R. Best and A. D. Yaghjian, “The Lower Bounds on  $Q$  for Lossy Electric and Magnetic Dipole Antennas,” *IEEE Antennas and Wireless Propagation Letters*, **3**, December 2004, pp. 314-316.
5. L. J. Chu, “Physical Limitations of Omni-directional Antennas,” *Journal of Applied Physics*, **19**, December 1948, pp. 1163-1175.

6. R. E. Collin and R. Rothchild, "Evaluation of Antenna  $Q$ ," *IEEE Transactions on Antennas and Propagation*, **AP-12**, January 1964, pp. 23-27.

7. M. Gustafsson, C. Sohl, and G. Kristensson, "Physical Limitations on Antennas of Arbitrary Shape," *Proceedings of the Royal Society A*, **463**, 2086, 2007, pp. 2589-2607.

8. G. A. Mavridis, D. E. Anagnostou, C. G. Christodoulou and M. T. Chryssomallis, "Quality Factor  $Q$  of a Miniaturized Meander Microstrip Patch Antenna," IEEE International Symposium on Antennas and Propagation, July 5-11, 2008, pp. 1-4.

9. G. A. Mavridis, C. G. Christodoulou and M. T. Chryssomallis, "Area Miniaturization of a Microstrip Patch Antenna and the Effect on the Quality Factor  $Q$ ," IEEE International Symposium on Antennas and Propagation, June 9-15, 2007, pp. 5435-5438.

10. H. A. Wheeler, "Fundamental Limitations of Small Antennas," *Proceedings IRE*, **35**, December 1947, pp. 1479-1484.

11. H. A. Wheeler, "The Radiansphere Around a Small Antenna," *Proceedings IRE*, **47**, August 1959, pp. 1325-1331.

12. H. A. Wheeler, "Small Antennas," *IEEE Transactions on Antennas and Propagation*, **AP-23**, December 1975, pp. 462-469.

13. J. S. McLean, "A Re-Examination of the Fundamental Limits on the Radiation  $Q$  of Electrically Small Antennas," *IEEE Transactions on Antennas and Propagation*, **AP-44**, 5, May 1996, pp. 672-676.

14. R. C. Hansen, "Fundamental Limitations in Antennas," *Proceedings IEEE*, **69**, February 1981, pp. 170-182.

15. D. Nyberg, P.-S. Kildal, and J. Carlsson, "Effects of Intrinsic Radiation  $Q$  on Mismatch Factor of Three Types of Small Antennas: Single-Resonance, Quadral-Transition and Cascaded-Resonance Types," *IET Microwaves, Antennas & Propagation*, **4**, 1, January 2010, pp. 83-90.

16. P. S. Kildal and S. R. Best, "Further Investigations of Fundamental Directivity Limitations of Small Antennas with and Without Round Planes," IEEE Antennas and Propagation Society International Symposium, July 5-11, 2008, pp. 1-4.

17. O. Quevedo-Teruel, E. Pucci and E. Rajo-Iglesias, "Compact Loaded PIFA for Multifrequency Applications," *IEEE Transactions on Antennas and Propagation*, **AP-58**, 3, March 2010, pp. 656-664.

18. D. E. Anagnostou, A. A. Gheethan, T. Amert, and K. W. Whites, "A Low-cost WLAN "Green" PIFA Antenna on Eco-Friendly Paper Substrate," IEEE International Symposium on Antennas and Propagation, June 1-5, 2009, pp. 1-4.

## Introducing the Authors



**Georgios A. Mavridis** was born in Serres, Greece, in July 1980. He received the Diploma (MSc equivalent) in Electrical and Computer Engineering from Democritus University of Thrace, Greece, in 2003. He is currently working toward his PhD degree in Electrical Engineering at the Democritus University of Thrace, Greece, in the area of miniaturization and improvement of the performance of printed electrically small antennas.

His research interests include printed electrically small antennas, antenna miniaturization, diversity antennas and techniques, reconfigurable RF devices, and smart antennas. He has published several journal and conference papers. He was awarded the "Excellence in Telecommunication Award" by Ericsson for his Diploma Thesis. He is a member of the Technical Chamber of Greece.



**Dimitris E. Anagnostou** received the BSEE from the Democritus University of Thrace, Greece, in 2000, and the MSEE and PhD degrees from the University of New Mexico in 2002 and 2005, respectively. From 2005 to 2006, he was a Post-Doctoral Fellow at the Georgia Institute of Technology, Atlanta, GA. Since 2007, he has been an Assistant Professor of Electrical and Computer Engineering at the South Dakota School of Mines and Technology, Rapid City, SD. He has published 60 peer-reviewed journal and conference papers. His current interests include reconfigurable and autonomous antennas and arrays, analytical methods for antenna design, electrically small antennas, flexible arrays, metamaterial-inspired antennas and microwave circuits, antenna miniaturization, eco-friendly ("green") RF harvesters and RF electronics, direct-write antennas, artificial dielectrics, antennas on solar cells, wireless sensors, RF-MEMS, propagation in tunnels, and microwave packaging.



Dr. Anagnostou received the 2011 DARPA Young Faculty Award and a 2011 AFRL ASEE Summer Faculty Fellowship. He also received the 2010 IEEE John Kraus Antenna Award from the IEEE Antennas and Propagation Society, along with his collaborators. He holds one patent on reconfigurable antennas. In 2006, he was also recognized as a distinguished scientist living abroad by the Hellenic Ministry of Defense. He serves as Associate Editor for the *IEEE Transactions on Antennas and Propagation* and the Springer *International Journal of Machine Learning and Cybernetics*. He was a member of the TPC and a session chair for the IEEE International Symposium on Antennas and Propagation. He has been a reviewer for 14 international publications. He has given two workshop presentations at IEEE AP-S and IEEE MTT-S International Symposia. Dr. Anagnostou is a member of Eta Kappa Nu, ASEE, and of the Technical Chamber of Greece, and a Senior Member of the IEEE.



**Michael T. Chryssomallis** received the Diploma in Electrical Engineering from Democritus University of Thrace, Greece, in 1981 and the PhD degree in Electrical Engineering from the same university in 1988. In 1982, he joined Democritus University as a Scientific Collaborator and he is currently an Associate Professor.

He worked with the Communications Group (Director, Prof. P. S. Hall) of the University of Birmingham for the period of October 1997 to January 1998 in the areas of active antennas, and with the Wireless Group (Director Prof. C. G. Christodoulou) of the University of New Mexico for the periods of April to June 2000, and April to July 2002, in the areas of microstrip antennas and arrays, and smart antennas. His current research interests are in the areas of small antennas, RF-MEMS, smart antennas, algorithms of beamforming and angle-of-arrival estimation, and propagation-channel characterization. He is the author or co-author of 60 journal papers and conference proceedings. He serves as a reviewer for several publications of the IEEE and IEE. He is a Senior Member of the IEEE. 